Photoneutron cross section measurements on the $N = 82$ nuclei ^{139}La and ^{141}Pr: Implications for *p*-process nucleosynthesis

H. Utsunomiya,[1] A. Makinaga,[1] S. Goko,[1] T. Kaihori,[1] H. Akimune,[1] T. Yamagata,[1] M. Ohta,[1] H. Toyokawa,[2] S. Müller,[3] Y.-W. Lui,[4] and S. Goriely[5]

[1]*Department of Physics, Konan University, Okamoto 8-9-1, Higashinada, Kobe 658-8501, Japan*

[2]*National Institute of Advanced Industrial Science and Technology, 1-1-1 Umezono, Tsukuba, Ibaraki 305-8568, Japan*

[3]*Institut fuer Kernphysik, TU Darmstadt, Schlossgartenstr 9, D-64289 Darmstadt, Germany*

[4]*Cyclotron Institute, Texas A&M University, College Station, Texas 77843, USA*

[5]*Institute d'Astronomie et d'Astrophysique, Université Libre de Bruxelles, Campus de la Plaine, CP-226, 1050 Brussels, Belgium*

(Received 23 September 2005; revised manuscript received 5 January 2006; published 22 August 2006)

Cross sections of the ^{139}La(γ, n) and ^{141}Pr(γ, n) reactions were measured using quasi-monochromatic γ-ray beams from laser Compton scattering. The results are compared to the predictions of Hauser-Feshbach statistical calculations using different models for the γ-ray strength function. The model parameters are constrained by the present experimental data and used to estimate the stellar photoneutron rates and their associated uncertainties and to study the implication for the production of the rare odd-odd nuclide ^{138}La by the p process. No evidence for a large thermonuclear p-process contribution to the solar ^{138}La is found. The need to further explore the photodestruction rate of ^{138}La is emphasized.

DOI: 10.1103/PhysRevC.74.025806 PACS number(s): 25.20.−x, 26.30.+k, 27.60.+j, 97.10.Tk

I. INTRODUCTION

The origin of the rare nuclide ^{138}La remains one of the key questions that nucleosynthesis theory is still trying to answer. Because of its scarcity in the universe and the neutron deficiency of this odd-odd nucleus, ^{138}La has so far been considered a p-process nucleus. However, ^{138}La is underproduced in all p-process calculations performed so far [1,2]. In view of the low ^{138}La abundance, it has been attempted to explain its production by nonthermonuclear processes involving either stellar energetic particles [3] or neutrino-induced transmutations [2,4]. The former mechanism is predicted not to be efficient enough, while the latter through the ν_e capture on ^{138}Ba was shown by [2] to be so far the most efficient production mechanism of the solar ^{138}La. Despite its promising character, the neutrino scenario still suffers from astrophysics as well as nuclear/neutrino physics uncertainties. In addition, it cannot be excluded that a substantial fraction of the solar ^{138}La be of a thermonuclear origin if agents other than type-II Supernovae could have contaminated the solar system with p nuclides. In particular, sub-Chandraskhar White Dwarf explosions could be significant contributors [1,5].

The thermonuclear origin of ^{138}La is known to depend in a sensitive way on the competition between the ^{138}La production and the ^{138}La destruction by photodissociation. It is shown in [2] that a suitable ^{138}La production can be obtained by adequate changes in the corresponding nominal ^{139}La(γ, n) and ^{138}La(γ, n) rates. Because the level of required changes is relatively high, only experimental measurements can possibly confirm this assumption. One major goal of the present article is, therefore, to provide some experimental constraint on the ^{139}La$(\gamma, n)^{138}$La production rate.

The p-process nucleosynthesis in the ^{138}La region is further complicated by the theoretical difficulty of estimating the reaction rates in a hot astrophysics plasma. Under such conditions, the photoreaction rates in particular can be significantly different from those obtained under laboratory conditions, and the theoretical uncertainties affecting the prediction in particular of the $E1$ strength function may impact the nucleosynthesis calculations. This is even more so in the region of the $N = 82$ shell closure where some of the ingredients of the reaction rate calculation may not be following some phenomenological systematics. In particular, the width of the giant dipole resonance (GDR) is known to be affected by shell structures [6], though almost all prescriptions assume a smooth mass dependence. The present measurements of the photoneutron reaction cross sections on the $N = 82$ nuclei ^{139}La and ^{141}Pr can shed light on such a shell effect and therefore constrain the prediction of the corresponding rates.

All these reasons motivated new accurate measurements of the photoneutron cross section of ^{139}La and ^{141}Pr. In Sec. II, the experimental procedure is described. The data analysis and final determination of the photoneutron cross sections and corresponding error bars are outlined in Sec. III. In Sec. IV, the experimental results are compared with theoretical Hauser-Feshbach calculations and the predictions based on different prescriptions for the γ-ray strength functions are discussed. The stellar photoreaction rates predicted with different models are also estimated in Sec. IV and the astrophysics implications discussed. Conclusions are drawn in Sec. V.

II. EXPERIMENTAL PROCEDURE

Photoneutron cross-section measurements on ^{139}La and ^{141}Pr were performed at the National Institute of Advanced Industrial Science and Technology (AIST). The experimental procedure was similar to that described in [7,8]. Since one can find detailed information in the literature, we here give a brief description of the experimental procedure. Metallic ^{139}La (99.9%) and ^{141}Pr (99.9%) targets 20 mm in diameter and 4 mm in thickness are irradiated with laser Compton scattering

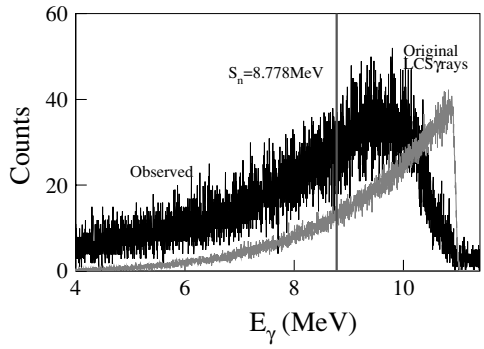

FIG. 1. Energy distribution of the LCS photons measured with a 120% relative efficiency germanium (HPGe) detector (the thick line). An incident photon spectrum (the thin line) that best reproduces the response function of the HPGe detector was obtained through a Monte Carlo analysis. The neutron separation energy of ^{139}La is indicated by a vertical line.

(LCS) γ-ray beams [9] at energies ranging from 9.10 to 14.01 MeV. Compton backscattering plays the role of a *photon accelerator*. The LCS γ-ray beam is produced in head-on collisions of laser photons from a Nd:YLF Q-switch laser in the second harmonics ($\lambda = 527$ nm) at a frequency of 1 KHz with relativistic electrons in the storage ring TERAS. The electron beam energy is tuned from 506.9 to 630.3 MeV. The Compton-backscattered γ rays are collimated into a pencil-like beam 2 mm in diameter with a 20-cm-thick lead collimator. The γ-ray flux was of the order of 10^4 counts per second.

Figure 1 shows the energy distribution of the LCS γ-ray beam measured with a 120% HPGe detector. The energy is calibrated with natural radioactivities, ^{40}K and ^{208}Tl. The energy spectrum of the incident LCS γ-ray beam obtained by a Monte Carlo analysis of the energy distribution [7] with the code EGS4 [10] is also shown in Fig. 1 (thin line). The energy spread of the LCS γ beam on the low-energy side is determined by the collimation and the electron beam emittance. The effect of the 2-mm collimation on the energy spread was comparable to that of the beam emittance, allowing a tighter collimation to reduce the energy spread at the cost of the γ flux. Photoreactions are induced by a fraction of LCS γ rays above the neutron threshold. During an exponential decay of the electron beam current with a lifetime of $\sim$6 h, the electron beam size in the region of the laser photon–electron interaction tended to decrease with time because of a space-charge effect, producing a time variation of the energy spread. The measurements that last less than an hour are found to be virtually free from this effect, but for longer runs near the neutron threshold the effect is clearly observed.

Neutrons are moderated by a polyethylene and detected with the double rings made of a total of 16 ^{3}He proportional counters. Background neutrons are identified as a time-independent component in a moderation-time distribution. The average energy of neutrons is determined by the ring ratio [7,11], which is the ratio of the number of neutrons detected by the inner ring (made of 8 ^{3}He counters) to that of the outer ring. The efficiencies of the two rings along with the sum efficiency are calibrated with a standard ^{252}Cf source and calculated as a function of neutron energy with the Monte Carlo simulation code MCNP [12].

LCS γ rays are monitored with a NaI(Tl) detector 8 in. in diameter and 12 in. in length. Pile-up spectra measured with the NaI(Tl) detector are used to determine the average number of LCS γ rays per pulse of the LCS beam [7].

The systematic uncertainty for the measured cross section is between 5.8 and 7.2%, as determined by the neutron detection efficiency (5%), the number of incident LCS γ rays (3%), and the electron beam size effect ($\lesssim$4.2%).

III. DATA REDUCTION

It is straightforward to determine cross sections in photonuclear reactions induced by monochromatic γ rays. The number of reactions induced by the photons in the target region $x \sim x + dx$ is $dY(x) = N_\gamma e^{-\mu x}\rho_t \sigma dx$, where N_γ is the number of incident photons, μ is the linear attenuation coefficient of photons in the target material, ρ_t is the number of target nuclei per unit volume, and σ is the photoreaction cross section. Integrating up to the target thickness t yields $Y = N_\gamma \sigma N_t f$, where N_t is the number of target nuclei per unit area ($N_t = \rho_t t$), and $f = (1 - e^{-\mu t})/(\mu t)$.

Thus, in (γ, n) reactions, the cross section is given by

$$\sigma(E_\gamma) = \frac{n_n}{N_t N_\gamma(E_\gamma) f \epsilon_n}. \tag{1}$$

Note that $Y = n_n/\epsilon_n$, where n_n is the number of detected neutrons and ϵ_n the neutron detection efficiency.

In reactions induced by nonmonochromatic γ rays, $N_\gamma(E_\gamma)\sigma(E_\gamma)$ in Eq. (1) must be replaced by the integral $\int n_\gamma(E)\sigma(E)dE$, where $n_\gamma(E)$ is the photon energy distribution, so that

$$\int_{S_n} n_\gamma(E)\sigma(E)dE = \frac{n_n}{N_t f \epsilon_n}. \tag{2}$$

μ does not significantly change within the energy spread of photons [13]; neither does $n_\gamma(E)$ in the course of passing through the target materials.

To determine the cross section at a given representative energy, E_R, Eq. (2) can be expanded in a Taylor series

$$\begin{aligned}\sigma(E_\gamma) = {} & \sigma(E_R) + \sigma^{(1)}(E_R)(E_\gamma - E_R) \\ & + \tfrac{1}{2}\sigma^{(2)}(E_R)(E_\gamma - E_R)^2 \\ & + \tfrac{1}{6}\sigma^{(3)}(E_R)(E_\gamma - E_R)^3 + \cdots,\end{aligned} \tag{3}$$

where $\sigma^{(i)} = d^i\sigma(E)/dE$. When the average energy $E_{\rm av}$ is chosen for E_R, the integral is given by

$$\int n_\gamma(E)\sigma(E)dE = N_\gamma\{\sigma(E_{\rm av}) + s_2(E_{\rm av}) + s_3(E_{\rm av}) + \cdots\}, \tag{4}$$

where $s_2(E_{\rm av}) = \frac{1}{2}N_\gamma\sigma^{(2)}(E_{\rm av})[\bar{E_\gamma^2} - E_{\rm av}^2]$ and $s_3(E_{\rm av}) = \frac{1}{6}N_\gamma\sigma^{(3)}(E_{\rm av})[\bar{E_\gamma^3} - 3E_{\rm av}\bar{E_\gamma^2} + 2E_{\rm av}^3]$ with $\bar{E_\gamma^i} = \int n_\gamma(E_\gamma) E_\gamma^i dE_\gamma/N_\gamma$. Note that $s_1(E_{\rm av})$ including the first derivative term $\sigma^{(1)}$ vanishes.

Substituting Eq. (4) into Eq. (2) yields

$$\sigma(E_{\rm av}) + s_2(E_{\rm av}) + s_3(E_{\rm av}) + \cdots = \frac{n_n}{N_{\rm t} N_\gamma(E_\gamma) f \epsilon_{\rm n}}. \quad (5)$$

Therefore the full Taylor series on the left-hand side of Eq. (5) can be determined from the experimental quantities $(n_n, N_t, N_\gamma, f, \varepsilon_n)$ on the right-hand side. By comparing Eqs. (1) and (5), one can see that when the average energy is used as a representative energy the monochromatic approximation [Eq. (1)] is derived from Eq. (5) by neglecting the higher-order terms in the Taylor series.

To determine the cross section at the average energy (the first term in the Taylor series in Eq. (5), the derivatives $[\sigma^{(i)}(E_{\rm av})]$ in the higher-order terms $(i = 2, 3, 4, \cdots)$ need to be evaluated numerically. The evaluation requires the energy dependence of the cross section, which is unknown until the cross section is determined. Therefore, an iterative evaluation is inevitable. First, one takes the monochromatic approximation by neglecting the higher-order terms in the Taylor series in Eq. (5) to obtain the cross section. The resultant energy dependence of the cross section is used for the first-step evaluation of $\sigma^{(i)}(E_{\rm av})$. After correction, the new cross section provides the energy dependence for the next iterative step, the procedure being performed until convergence is achieved.

The energy dependence is obtained by fitting the cross section data with the following formula near the neutron threshold [14,15] plus a third-order polynomial:

$$\sigma(E) = \sigma_0 \left(\frac{E_\gamma - S_n}{S_n} \right)^p. \quad (6)$$

Here S_n is the neutron separation energy and the power p is related to the orbital angular momentum of the emitted neutrons ℓ by $p = \ell + 1/2$. s- and p-wave neutrons may suffice for reactions near the neutron threshold. But for a possible mixture of s and p waves, p should be treated as an experimental parameter together with σ_0.

Since the Taylor series of Eq. (6) diverges for an s-wave emission ($p = 1/2$), a spline fit with third-order polynomials [16] was carried out by dividing the best-fit curve into 375 equi-energy bins in the region from threshold to 12.53 MeV for ^{139}La. The spline fit ensured that the individual polynomials were connected smoothly at every boundary of the energy bins.

The iterative correction converged fast at a level $\ll 1\%$. The resultant cross sections at the average energies are shown in Fig. 2. In comparison with those in the monochromatic approximation (open circles), the corrections for the higher-order terms in the Taylor series amount to 1.0%–5.8% in the low-energy region of astrophysical importance ($\leqslant$10.05 MeV), while they amount to 4.0%–38% at higher energies.

IV. RESULTS

The measured (γ, n) cross sections for ^{139}La and ^{141}Pr are shown in Fig. 3 in comparison with the existing data obtained with the positron annihilation γ rays [17–20] and betatron bremsstrahlung [21] (for more references, see [22]). The positron annihilation in flight produced quasi-monochromatic

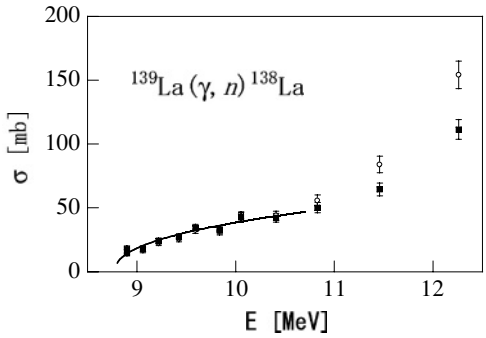

FIG. 2. Photoneutron cross sections for ^{139}La at the average LCS photon energies (the solid circles) in comparison with those in the monochromatic approximation (the open circles). The best-fit to the solid circles with Formula (6) is shown by the solid line.

γ rays accompanied by a continuous positron bremsstrahlung. Contributions from the bremsstrahlung were experimentally simulated and subtracted by using electron beams. The subtraction can be a source of uncertainties in absolute cross sections [8]. On the other hand, in the bremsstrahlung measurement [21] experimental yield curves were deconvoluted by one of regularization methods [23] assuming the smoothness of the cross section. The resultant cross section may have been subject to the chosen "regularizator" of the unfolding method [22].

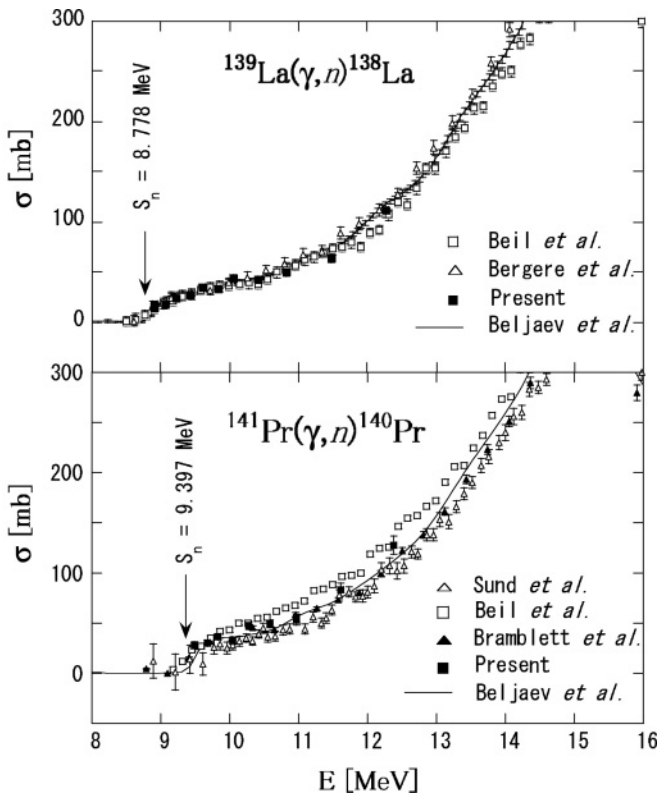

FIG. 3. Photoneutron cross sections for ^{141}Pr and ^{139}La. The previous data obtained with photon sources of in-flight positron annihilation [17–20] and bremsstrahlung [21] are also shown for comparison.

Previously the cross sections for ^{141}Pr measured by using the position annihilation γ rays showed a persistent difference [17,19,20]. While the two data sets obtained with the BF_3 counters embedded in the paraffin moderator [17] and by photoactivation [20] agree well, their cross sections are smaller than those obtained with the gadolinium-doped liquid scintillator tank [19], producing a GDR peak at a slightly high energy. The bremsstrahlung data [21] for ^{141}Pr are similarly characterized by smaller cross sections in the low-energy region, but are consistent with the data of [19] in the peak region. The present data for ^{141}Pr show some enhancement from the data of [17,20] near the neutron threshold though the enhancement may not be as large as that of [19], being rather consistent with that of [21]. As for ^{139}La, it turned out that the present data are very consistent with the positron annhilation data [18,19] as well as the bremsstrahlung data [21].

The best fit to the present cross section with Eq. (6) gives $p = 0.43 \pm 0.06$ and $\sigma_0 = 90 \pm 14$ mb for the ^{139}La(γ, n) reaction and $p = 0.29 \pm 0.06$ and $\sigma_0 = 88 \pm 13$ mb for the ^{141}Pr(γ, n) reaction.

Since the integral in Eq. (2) is an experimental quantity, the parameters σ_0 and p in Eq. (6) can directly be determined by means of a least-squares fit to a set of experimental values of the integral. This analysis provides the best-fit formula with $p = 0.43^{+0.05}_{-0.03}$ and $\sigma_0 = 98 \pm 10$ mb for ^{139}La and $p = 0.32 \pm 0.03$ and $\sigma_0 = 97 \pm 8$ mb for ^{141}Pr, respectively. These agree with the preceding results from the fit to the cross-section data within the uncertainties.

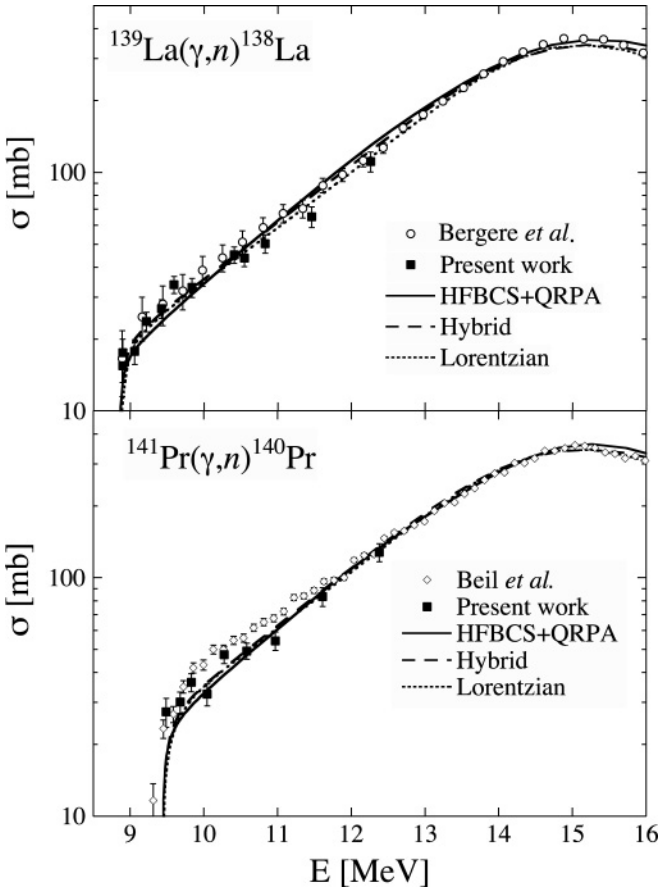

FIG. 4. Comparison between measured and calculated photoneutron cross sections for ^{139}La(γ, n) (upper panel) and ^{141}Pr(γ, n) (lower panel). The previous data for ^{139}La [18] and ^{141}Pr [19] are also shown for comparison. The different theoretical predictions are described in the text.

V. DISCUSSION OF THE EXPERIMENTAL RESULTS

A. Comparison with theory

The cross sections measured in the present work are now compared with the predictions of the Hauser-Feshbach (HF) compound nucleus theory [24], making use of different nuclear inputs in the estimation of the transmission coefficients. To estimate the reliability and accuracy of the calculated stellar rates, it is indeed of interest to analyze to what extent different models adjusted to the same experimental data set provide different predictions of the stellar rates.

The key ingredient to understand the photoemission data concerns the γ-ray strength function. We consider here two different phenomenological models, namely, the Lorentzian model [25] which considers a width $\Gamma(E) = \Gamma_{\rm GDR}\sqrt{E/E_{\rm GDR}}$ and the Hybrid model [26] which couples the energy-dependent-width GDR Lorentzian description at high energies with an analytical approximation to the theory of finite Fermi systems at energies below the neutron separation energy [27]. Although both prescriptions are rather similar, the extrapolation of the strength functions at low energies can differ in a non-negligible way. In addition to the Lorentzian-type approaches, the quasi-particle random phase approximation (QRPA) model of [28] is also considered here for estimating the photon transmission coefficients.

As far as the other ingredients to the Hauser-Feshbach formalism are concerned, the nuclear level densities are derived by default from the microscopic calculations taking into account the discrete structure of the single-particle spectra associated with HFBCS potentials [29]. To estimate the sensitivity to nuclear level densities, we also consider the widely used back-shifted Fermi gas model based on the global parametrization of [30]. The transmission coefficients for particle emission are calculated by default with the so-called JLMB semimicroscopic potential of [31], or for our sensitivity analysis with the global phenomenological mass- and energy-dependent potential of Woods-Saxon-type developed by [32].

In Fig. 4, we compare the present experimental data with the predictions obtained with three different prescriptions of the $E1$ strength functions, namely, the Lorentzian-type model [25], the Hybrid model [26], and the HFBCS+QRPA model [28]. These three GDR models are, however, tuned to reproduce the GDR peak energy ($E_{\rm GDR}$) of about 15.2 and 15.4 MeV, the full-width at half maximum, and the peak cross section of about 340 and 350 mb for ^{139}La and ^{141}Pr, respectively. While the location and peak cross section follow a rather smooth trend in this region of the nuclear chart, the GDR width is known to be affected by the shell structure around the magic number $N = 82$. The shell-dependent part of the GDR width can be attributed to the coupling between dipole oscillations

and surface vibrations [6]. The magic nuclei being the stiffest against surface vibrations, they are characterized by a smaller width. If not available experimentally, the GDR width can be derived from the prescription [6] that includes a droplet one-body damping contribution and a broadening term resulting from the coupling of dipole mode and surface vibrations. In the present case, the GDR width is directly determined for each model by a direct fit to the experimental data. It should, however, be kept in mind that to each formula corresponds a different parametrized width $\Gamma_{\rm GDR}$ due to the different energy-dependence adopted for the $E1$ strength function.

As seen in Fig. 4, the three GDR models considered here reproduce the experimental data almost identically and therefore give rise to similar estimates for the photodissociation rate on the target in its ground state. At a typical p-process temperature of $T = 2.5 \times 10^9$ K, we find a rate $\lambda^0_{(\gamma,n)} = 0.18 \pm 0.02$ s^{-1} for ^{139}La and $\lambda^0_{(\gamma,n)} = 0.015 \pm 0.004$ s^{-1} for ^{141}Pr, where the quoted uncertainties are associated with the adopted model for the $E1$ strength function, nuclear level densities, and optical potential. The errors are seen not to exceed some 10% and 30%, respectively.

When considering the total stellar rate, the contribution of the thermally populated state becomes dominant at temperatures of interest for the p-process nucleosynthesis, so that the photodissociation rate becomes sensitive to the tail of the γ-ray strength below the neutron threshold. These new conditions relax somehow the constraints related to experimental cross-section measurements above the neutron threshold. At $T = 2.5 \times 10^9$ K, we found stellar rates $\lambda^*_{(\gamma,n)} = 27 \pm 15$ s^{-1} for ^{139}La and 4.5 ± 3 s^{-1} for ^{141}Pr. These rates are about 100 times larger than those for the targets in their ground state. The uncertainties are also by far larger than those obtained under the laboratory conditions and largely originate from the different energy dependences prescribed by the three different models of the γ-ray strength function. This is illustrated in Fig. 5 for the ^{139}La case. The three models give similar results at energies above the neutron threshold (i.e., $E \gtrsim 9$ MeV), since they are all tuned to the (γ, n) data. However, at low energies, significant discrepancies arise and are responsible for the above-quoted error bars. This result stresses the need to further explore experimentally as well as theoretically the low-energy E1 strength below the neutron threshold.

B. Astrophysics implications

As discussed in Sec. I and Ref. [2], the puzzling thermonuclear production of the rare odd-odd ^{138}La depends in a sensitive way on the competition between the ^{138}La production and the ^{138}La destruction by photodissociation. In Ref. [2], like in all previous p-process simulations, the thermonuclear mechanisms entering the p-process nucleosynthesis can not be considered to be totally responsible for the solar ^{138}La. A larger p-process abundance of ^{138}La can be achieved, however, by a significant increase in the ^{139}La$(\gamma, n)^{138}$La production rate and/or a decrease in the ^{138}La$(\gamma, n)^{137}$La destruction rate with respect to some standard values. The standard values obtained in Ref. [2] were predicted by the Hauser-Feshbach code MOST and amount to $\lambda^*_{(\gamma,n)} = 12$ s^{-1} for ^{139}La (which corresponds to the lower limit estimated in the previous subsection) and 1200 s^{-1} for ^{138}La at $T = 2.5 \times 10^9$ K. From the present analysis, an increase by a factor of 3.5 to reach the upper value of $\lambda^*_{(\gamma,n)} \simeq 42$ s^{-1} found in Sec. V A cannot be excluded when considering other nuclear inputs to the Hauser-Feshbach model, i.e., more precisely, the Lorentzian-type E1 strength function [25].

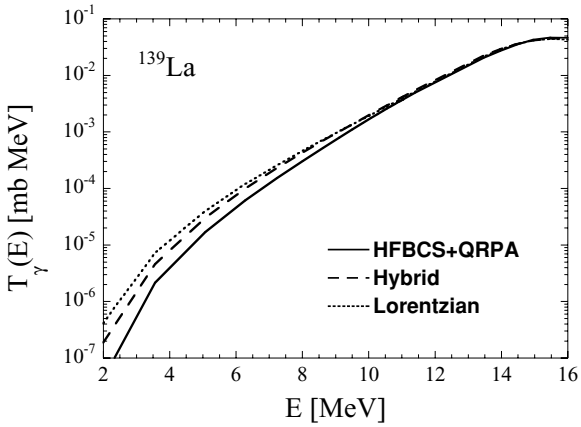

FIG. 5. Comparison of the ^{139}La total $E1$ transmission coefficients predicted by the three models adopted in the present work.

The p-process ^{138}La abundance also depends on the ^{138}La$(\gamma, n)^{137}$La destruction rate. In this case, no experimental data exist, neither to constrain the E1 strength function nor the nuclear level densities. We estimate $\lambda^*_{(\gamma,n)}(^{138}\text{La})$ to be in the range of 500 to 3000 s^{-1}. It should, however, be emphasized that by consistency the same model for the E1 strength function should be used to determine both the ^{138}La production and the ^{138}La destruction rates. The above-mentioned upper limit for the production rate implies a simultaneous increase in the destruction rate with respect to the above-quoted value of 1200 s^{-1}. It is therefore unlikely that an increase in the ^{138}La production be accompanied by a simultaneous decrease in the ^{138}La destruction. Hence, based on Fig. 2 of Ref. [2], the photoreaction mechanisms are not favored to explain the total ^{138}La solar abundance. However, at this stage, no definite conclusion can be drawn because of the large uncertainties still affecting the unconstrained stellar photoneutron rate of ^{138}La. Future experiments on the ^{138}La nuclear properties will hopefully bring new insight.

VI. CONCLUSION

Photoneutron cross sections were measured for ^{139}La and ^{141}Pr using quasi-monochromatic γ-ray beams from laser Compton scattering. The present experimental results confirm the measurements obtained previously by other techniques. The cross sections are used to constrain the model parameters in the framework of the Hauser-Feshbach model. Different sets of nuclear ingredients are adopted to estimate the photoneutron cross sections. Although the present data strongly constrained the stellar rate on the ground-state target, the thermal population of the target state in the astrophysics plasma makes the contribution of the excited state dominant, so that the stellar

rate becomes sensitive to the experimentally unknown γ-ray strength below the neutron threshold. A factor of 2 uncertainty remains on the stellar rate at typical p-process temperatures. Although there is no evidence for a large thermonuclear contribution to the ^{138}La p-process solar abundance, decisive conclusions will first require new experimental explorations, in particular regarding the nuclear properties of the rare ^{138}La nuclide.

ACKNOWLEDGMENTS

We thank T. Hayakawa and T. Shizuma for their cooperation in the early stage of this research. This work was supported by the Japan Private School Promotion Foundation and the Japan Society of the Promotion of Science. S.M. was supported by the DFG (SFB634). S.G. is a FNRS Research Associate.

[1] M. Arnould and S. Goriely, Phys. Rep. **384**, 1 (2003).
[2] S. Goriely, M. Arnould, I. Borzov, and M. Rayet, Astron. Astrophys. **375**, L35 (2001).
[3] J. Audouze, Astron. Astrophys. **8**, 436 (1970).
[4] S. E. Woosley, D. H. Hartmann, R. D. Hoffman, and W. C. Haxton, Astrophys. J. **356**, 272 (1990).
[5] S. Goriely, J. José, M. Hernanz, M. Rayet, and M. Arnould, Astron. Astrophys. **383**, L27 (2002).
[6] F.-K. Thielemann and M. Arnould, in *Proceedings of Conference on Nuclear Data for Science and Technology*, edited by K. Böckhoff (Reidel, Dordrecht, 1983), p. 762.
[7] H. Utsunomiya, H. Akimune, S. Goko, M. Ohta, H. Ueda, T. Yamagata, K. Yamasaki, H. Ohgaki, H. Toyokawa, Y.-W. Lui, T. Hayakawa, T. Shizuma, E. Khan, and S. Goriely, Phys. Rev. C **67**, 015807 (2003).
[8] T. Shizuma, H. Utsunomiya, P. Mohr, T. Hayakawa, S. Goko, A. Makinaga, H. Akimune, T. Yamagata, M. Ohta, H. Ohgaki, Y.-W. Lui, H. Toyokawa, A. Uritani, and S. Goriely, Phys. Rev. C **72**, 025808 (2005).
[9] H. Ohgaki, S. Sugiyama, T. Yamazaki, T. Mikado, M. Chiwaki, K. Yamada, R. Suzuki, T. Noguchi, and T. Tomimasu, IEEE Trans. Nucl. Sci. **38**, 386 (1991).
[10] W. R. Nelson, H. Hirayama, and W. O. Roger, The EGS4 Code Systems, SLAC-Report-265, 1985.
[11] B. L. Berman, J. T. Caldwell, R. R. Harvey, M. A. Kelly, R. L. Bramblett, and S. C. Fultz, Phys. Rev. **162**, 1098 (1967).
[12] J. F. Briesmeister, computer code MCNP, Version 4C, Los Alamos National Laboratory, Los Alamos, 2000.
[13] J. H. Hubbell and M. J. Berger, Chap. 4 *Engineering Compendium on Radiation Shielding*, Vol. 1, *Shielding Fundamentals and Methods*, edited by R. G. Jaeger, E. P. Blizard, A. B. Chilton, M. Grotenhuis, A. Hönig, Th. A. Jaeger, and H. H. Eisenlohr (Springer-Verlag, New York, 1968), p. 175.
[14] E. P. Wigner, Phys. Rev. **73**, 1002 (1948).
[15] G. Breit, Phys. Rev. **107**, 1612 (1958).
[16] P. R. Bevington and D. K. Robinson, *Data Reduction and Error Analysis for the Physical Sciences, Second Edition* (McGraw–Hill Inc., New York, 1992), p. 228.
[17] R. L. Bramblett, J. T. Caldwell, B. L. Berman, R. R. Harvey, and S. C. Fultz, Phys. Rev. C **148**, 1198 (1966).
[18] R. Bergère, H. Beil, and A. Veyssière, Nucl. Phys. **A121**, 463 (1968).
[19] H. Beil, R. Bergère, P. Carlos, A. Lepretre, and A. Veyssière, Nucl. Phys. **A172**, 426 (1971).
[20] R. E. Sund, V. V. Verbinski, H. Weber, and L. A. Kull, Phys. Rev. C **2**, 1129 (1970).
[21] S. N. Beljaev and V. A. Semenov, Izv. Akad. Nauk SSSR, Ser. Fiz. **55**, 953 (1991).
[22] Handbook on Photonuclear data for applications: Cross Sections and Spectra LAEA-Tecdoc-1178, 2000.
[23] V. F. Turchin, V. P. Kozlov, and M. S. Malkevich, Soviet Physics Uspekhi **13**, 681 (1971) [Usp. Fiz. Nauk **102**, 345 1970].
[24] M. Arnould and S. Goriely, Nucl. Phys. A (in press).
[25] C. M. McCullagh, M. L. Stelts, and R. E. Chrien, Phys. Rev. C **23**, 1394 (1981).
[26] S. Goriely, Phys. Lett. **B436**, 10 (1998).
[27] S. G. Kadmenskii, V. P. Markushev, and V. I. Furman, Sov. J. Nucl. Phys. **37**, 165 (1983).
[28] S. Goriely and E. Khan, Nucl. Phys. **A706**, 217 (2002).
[29] P. Demetriou and S. Goriely, Nucl. Phys. **A695**, 95 (2001).
[30] S. Goriely, J. Nucl. Sci. Technol. **Suppl. 2** (edited by K. Shibata), 536 (2002).
[31] E. Bauge, J. P. Delaroche, and M. Girod, Phys. Rev. C **63**, 024607 (2001).
[32] A. J. Koning, and J. P. Delaroche, Nucl. Phys. **A713**, 231 (2003).